Journal of Medicinal Chemistry Article

J. Med. Chem. **2009,** *52,* 6233–6243 **6233**
DOI: 10.1021/jm901036q

Structure−Brain Exposure Relationships in Rat and Human Using a Novel Data Set of Unbound Drug Concentrations in Brain Interstitial and Cerebrospinal Fluids

Markus Fridén,*[,†,‡] Susanne Winiwarter,[†] Gunilla Jerndal,[†] Ola Bengtsson,[†,‡] Hong Wan,[§] Ulf Bredberg,[†] Margareta Hammarlund-Udenaes,[‡] and Madeleine Antonsson[†]

[†]*Discovery DMPK, AstraZeneca R&D Mölndal, SE-431 83 Mölndal, Sweden,* [‡]*Department of Pharmaceutical Biosciences, Division of Pharmacokinetics and Drug Therapy, Uppsala University, Box 591, SE-751 24 Uppsala, Sweden, and* [§]*Lead Generation DMPK and Physical Chemistry, AstraZeneca R&D Mölndal, Mölndal, Sweden*

Received July 13, 2009

New experimental methodologies were applied to measure the unbound brain-to-plasma concentration ratio ($K_{p,uu,brain}$) and the unbound CSF-to-plasma concentration ratio ($K_{p,uu,CSF}$) in rats for 43 structurally diverse drugs. The relationship between chemical structure and $K_{p,uu,brain}$ was dominated by hydrogen bonding. Contrary to popular understanding based on the total brain-to-plasma concentration ratio (logBB), lipophilicity was not a determinant of unbound brain exposure. Although changing the number of hydrogen bond acceptors is a useful design strategy for optimizing $K_{p,uu,brain}$, future improvement of in silico prediction models is dependent on the accommodation of active drug transport. The structure−brain exposure relationships found in the rat also hold for humans, since the rank order of the drugs was similar for human and rat $K_{p,uu,CSF}$. This cross-species comparison was supported by $K_{p,uu,CSF}$ being within 3-fold of $K_{p,uu,brain}$ in the rat for 33 of 39 drugs. It was, however, also observed that $K_{p,uu,CSF}$ overpredicts $K_{p,uu,brain}$ for highly effluxed drugs, indicating lower efflux capacity of the blood−cerebrospinal fluid barrier compared to the blood−brain barrier.

1. Introduction

Centrally acting drugs are ideally designed with an intrinsic ability to circumnavigate the protective efflux systems of the blood−brain barrier (BBB[a]), ensuring an effective drug concentration in the brain at minimal doses. While all drugs do reach the brain to some extent, some drugs, including many CNS-active drugs, are effluxed from the brain, resulting in reduced brain concentrations and proportionally higher dose requirements. It is generally believed that CNS side effects associated with peripherally acting drugs are avoided if the drugs are kept out of the brain. Brain exposure, described as the steady-state unbound brain-to-plasma concentration ratio, $K_{p,uu,brain}$, is a significant pharmacological entity that quantifies the increased dosage required as a result of BBB efflux transport.[1,2] For peripherally acting drugs with potential CNS side effects, the $K_{p,uu,brain}$ is conceptually inversely related to the therapeutic window.

The level of unbound brain exposure is determined by the chemical structure of the drug and by interactions between the drug and transporters and membranes. It is therefore necessary to address the issue of unbound brain exposure when designing new, potentially improved chemical structures. Information is currently lacking on the association between specific chemical drug structures and the extent of *unbound* brain exposure, i.e., the chemical structure−brain exposure relationship. There are as yet insufficient experimental data in humans on which to build such models because of the invasive nature of the methods. While positron emission tomography (PET) can be useful for studies in humans, the only source of information on brain exposure in humans currently readily available is the drug concentration in samples of cerebrospinal fluid (CSF). A basic understanding of structure−brain exposure relationships, such as the importance of molecular size and polar surface area (PSA), has been obtained from analysis of the properties of drugs classified as CNS active or CNS inactive.[3−6] While there is no reason to dispute these findings, the view on brain exposure seems to have been that compounds are considered, perhaps simplistically, to either "penetrate" or "not penetrate"

*To whom correspondence should be addressed. Phone: +46 31 7065360. Fax: +46 31 7763786. E-mail: Markus.Friden@farmbio.uu.se.

[a] Abbreviations: A_{brain}, amount of drug in brain excluding vascular spaces (μmol/kg brain); ACDLogD7.4, calculated octanol−water partitioning coefficient at pH 7.4; ACDLogP, calculated octanol−water partitioning coefficient; BBB, blood−brain barrier; BCRP, breast cancer resistance associated protein; BCSFB, blood−cerebrospinal fluid barrier; $C_{brain,h}$, drug concentration in brain homogenate sample (μmol/kg brain); $C_{CSF,}$ total drug concentration in cerebrospinal fluid (μmol/L); $CL_{bulkflow}$, drug clearance by bulk flow of brain interstitial fluid; CL_{in}, blood−brain barrier influx clearance of a drug; $CL_{passive}$, passive blood−brain barrier transport clearance of a drug; $CL_{out,}$ blood−brain barrier efflux clearance of a drug; ClogP, calculated octanol−water partitioning coefficient; $C_{p,}$ total drug concentration in plasma (μmol/L); CNS, central nervous system; CSF, cerebrospinal fluid; $C_{u,CSF}$, unbound cerebrospinal fluid concentration (μmol/L); $C_{u,p}$, unbound drug concentration in plasma (μmol/L); $f_{u,p}$, unbound fraction of drug in plasma; $f_{u,CSF}$, unbound fraction of drug in cerebrospinal fluid; HBA, number of hydrogen bond acceptors; HBD, number of hydrogen bond donors; $K_{p,brain}$, total brain-to-plasma concentration ratio of a drug; $K_{p,uu,brain}$, unbound brain-to-plasma concentration ratio of a drug; $K_{p,uu,CSF}$, unbound cerebrospinal fluid-to-plasma ratio of a drug; logBB, logarithm of the total brain-to-plasma ratio, i.e., logarithm of $K_{p,brain}$; LogPS, logarithm of the blood−brain barrier permeability surface area product; LogUnionized, logarithm of the fraction of molecules that are un-ionized; MRP, multidrug resistance-associated protein; MW, molecular weight (Da); NPSA, van der Waals nonpolar surface area; OAT, organic anion transporter; OATP, organic anion transporting polypeptide; OCT, organic cation transporter; PCA, principal component analysis; Pgp, P-glycoprotein; PLS, projections to latent structures; PSA, van der Waals polar surface area; $Q_{alb,}$ cerebrospinal fluid-to-plasma concentration ratio of albumin; QSAR, quantitative structure−activity relationships; RingCount, number of rings in a molecule; rmse, root of mean squared error; RotBond, number of rotatable bonds; V_{eff}, effective vascular plasma space of a drug (μL/g brain); VIP, variable importance for projections; VOL, molecular volume; $V_{protein}$, apparent vascular space of plasma proteins (μL/g brain); $V_{u,brain}$, unbound brain volume of distribution (μL/g brain); V_{water}, apparent vascular space of plasma water (μL/g brain).

Published on Web 09/18/2009

the brain. In contrast, $K_{p,uu,brain}$ provides a quantitative, meaningful definition of brain exposure and a method for ranking and comparing compounds in drug discovery.

As discussed in a recent review on the topic,[7] structure−brain exposure relationships have for many years been derived from data on the total brain-to-plasma concentration ratio, $K_{p,brain}$, also known as logBB. The logBB value is, however, affected by the extent of plasma protein and brain tissue binding, which are processes unrelated to BBB transport and unbound brain exposure. Therefore, it is not possible to interpret logBB as a pharmacodynamic entity nor is it possible to (correctly) rank compounds. The widespread use of logBB not only demonstrates a lack of understanding that the unbound drug concentration drives BBB transport but also highlights the lack of methods for efficiently measuring unbound brain exposure. Moreover, the permeability of the BBB (logPS) has been suggested as a replacement for logBB for in silico predictions,[8] but the rate of transport into the brain is of little pharmacological consequence for the repeated dosing situation. The recent development and validation of brain homogenate binding[9,10] and brain slice methods[11−13] to measure unbound brain concentrations have contributed to the acceptance of $K_{p,uu,brain}$ as an important parameter in drug discovery.[7,14] However, although data sets of $K_{p,uu,brain}$ using the brain homogenate method are available,[10,15−21] there are, to the best of our knowledge, no published in silico models based on these new and more relevant data. This paper presents a study that was undertaken to re-evaluate the structure−brain exposure relationships for 43 compounds, resulting in an original in vivo data set for $K_{p,uu,brain}$ in the rat. The data set for these compounds is unique in that $K_{p,uu,brain}$ has been determined at steady state in a consistent manner using the brain slice method, which is more reliable than the brain homogenate method.[12] The study also sought to assess if these structure−brain exposure relationships are applicable to humans, by comparing the unbound cerebrospinal fluid−plasma concentration ratio ($K_{p,uu,CSF}$) in rats and human patients for the same set of compounds. In support of the cross-species comparison and in order to evaluate the utility of CSF as a surrogate measure of brain exposure, a comparison was made between $K_{p,uu,CSF}$ and $K_{p,uu,brain}$ within the rat. This comparison provided a platform for the analysis of the relative drug efflux and influx capacity of the blood−cerebrospinal fluid barrier (BCSFB) and the BBB.

2. Materials and Methods

2.1. Compound Selection. In 2004, Shen et al.[22] published a review of available clinical data on drug concentrations in the CSF for 92 drugs from 5 different therapeutic areas (CSF data set). This data set was used as a starting point for the selection of compounds, since one of the aims of the study was to relate the data obtained from rats to available human data. A separate data set of 24 diverse drugs represented the range of chemical structural space for drugs on the Swedish market[23] (diverse data set). The diverse data set was used as a template in order to ensure a representative selection of drugs from the CSF data set. Molecular descriptors (see section 2.3.1) were calculated for all compounds. A principal component analysis (PCA) using Simca-P+[24] was performed for the 24 drugs of the diverse data set. The 92 drugs of the CSF data set were projected onto this PCA, and 36 drugs were initially selected according to the resulting scores. Drugs with significant bioanalytical challenges were later replaced by similar drugs. Drugs of particular interest for the BBB were added even if they were not mentioned in Shen's review. The final data set consisted of 43 compounds, with human CSF data available for 32 compounds. Figure 1 shows the distribution of the selected compounds in comparison to the diverse data set and the CSF data set in the PCA score plot. The chemical structures of the 43 drugs are given as Supporting Information (Figure S1). The compounds included substrates of human P-glycoprotein (Pgp, MDR1), breast cancer resistance associated protein (BCRP), multidrug resistance-associated proteins (MRPs), organic anion transporters (OATs), organic anion transporting polypeptide (OATPs), and organic cation transporters (OCTs) (Supporting Information, Table S1).

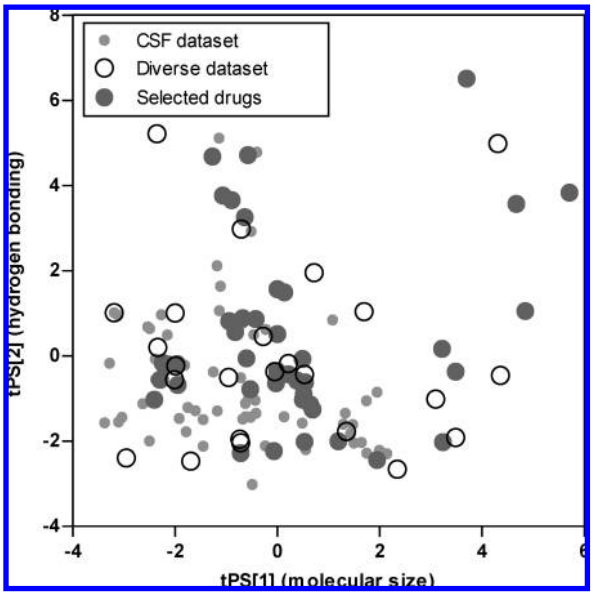

Figure 1. PCA score plot of the CSF data set,[22] diverse data set, and the selected drugs. Principal components 1 (tPS[1]) and 2 (tPS[2]) represent the molecular descriptor related to molecular size and hydrogen bonding (polarity), respectively.

2.2. Measurement of Unbound Brain Exposure in the Rat: $K_{p,uu,brain}$ and $K_{p,uu,CSF}$. 2.2.1. Chemicals. 2-Ethyl-2-phenylmalonamide was purchased from Acros Organics (Geel, Belgium). Amitriptyline and thioridazine were purchased from ICN Biomedicals (Eschwege, Germany). Delavirdine and gabapentin were purchased from Toronto Research Chemicals Inc. (Toronto, Canada). Morphine, morphine-3-glucoronide, morphine-6-glucuronide, oxycodone, and oxymorphone were obtained from Lipomed (Arlesheim, Switzerland). Salicylic acid and tramadol were obtained from Fluka BioChemika (Poole, U.K.). Moxalactam and oxprenolol were purchased from MP Biomedicals Inc. (Illkirsch, France). Nelfinavir mesylate was purchased from Apin Chemicals (Abingdon, U.K.). All other drugs were purchased from Sigma (St. Louis, MO).

2.2.2. Drug Administration and Sampling of CSF, Brain, and Plasma. All studies were approved by the Animal Ethics Committee of Gothenburg University (412-2005, 169-2006, 221-2008). The femoral vein of male Sprague−Dawley rats (Harlan, Horst, The Netherlands) weighing 250−350 g was surgically catheterized at least 24 h prior to the experiment. The drugs were administered in cassettes of two to three drugs as 4 h constant-rate intravenous infusions to approach steady state, using a flow rate of 1 (mL/kg)/h, corresponding

to dosage rates of 2 (μmol/kg)/h for each drug. Each cassette was given to a separate group of rats. The cassettes were designed to enable simultaneous analysis of the drugs. The dosage was kept low, at 2 (μmol/kg)/h, in order to minimize the risk of interactions between the compounds at the BBB. The vehicle used was saline or a 1:1:1 (w/w/w) mixture of dimethylacetamide, tetraethylene glycol, and water. At the end of the infusion, the rats were anesthetized by inhalation of isoflurane, and CSF (50 μL) was collected by puncturing the cisterna magna using a fine needle connected to a cannula. The CSF sample was dispensed from the cannula into a 96-deep-well plate containing 5 μL of blank plasma, followed by rinsing three times with 50 μL of methyl *tert*-butyl ether/hexane (1:1) to minimize adsorption of lipophilic drugs to the walls of the catheter. Immediately after CSF sampling, a blood sample (~2 mL) was collected in a heparinized tube from the abdominal aorta, followed by immediate severing of the heart. The brain was removed, and a coronal section (6 mm) containing striatum was cut and divided into smaller pieces. A brain sample (350−375 mg) was transferred to an Eppendorf tube and homogenized in three volumes of deionized water using an ultrasonic probe (Branson, Sonifier 250, Danbury, CT). All samples were stored at −20 °C until analysis by reversed phase liquid chromatography and multiple reaction monitoring mass spectrometry (LC−MS/MS).

The possible impact of the vehicle used on the permeability of the brain barriers was determined by studying the brain and CSF distribution of the permeability marker ^{14}C-sucrose. The study had two arms with respect to the vehicle. One group of six animals was given the radioactive isotope as a 4 h constant-rate infusion in the vehicle, and the other group was given the same dose in saline. Samples were obtained as described above, solubilized in 1 mL of Soluene-350 (Perkin-Elmer, Boston, MA) and decolorized with 100 μL of hydrogen peroxide. The radioactivity in the samples was measured using a liquid scintillation counter (Wallac Winspectral 1414, Turku, Finland) and an Opti-Phase "HiSafe 3" scintillation cocktail (Fisher Chemicals, Loughborough, U.K.).

2.2.3. Plasma Protein and Brain Tissue Binding: In Vitro. The unbound fraction in plasma ($f_{u,p}$) was measured using an equilibrium dialysis method.[25] Pooled plasma from all rats, with each of the rats given a cassette of drugs, was divided into three to five aliquots of 200 μL and dialyzed overnight against 200 μL of phosphate buffer (122 mM). A buffer pH of 7.0 was used in order to offset an upward shift in pH during the dialysis, resulting in a final pH of 7.4. Buffer and plasma samples were analyzed as described below.

The uptake and binding of drug in brain cells were estimated as the unbound brain volume of distribution ($V_{u,brain}$) using a brain slice method described previously in detail.[11] In short, freshly prepared 300 μm brain slices from drug-naive rats were incubated for 5 h in a buffer containing up to 10 drugs at very low concentrations (100 nM). The unbound drug concentration in the slice interstitial fluid was taken to be equal to the drug concentration in buffer. $V_{u,brain}$ (mL/g brain) was then calculated as the ratio of the amount of drug in the slice (nmol/g brain) to the measured final buffer concentration (μmol/L).

2.2.4. Bioanalytical Procedures. The drug concentration in all in vivo and in vitro samples was quantified using LC−MS/MS with positive or negative electrospray ionization. The LC−MS/MS system consisted of an LC-10AD pump (Schimadzu, Columbia, MA), a CTC HTS Pal autosampler (CTC Analytics, Zwingen, Switzerland), and a Micromass Ultima Platinum detector (Waters, Manchester, U.K.). Mass transitions and detailed chromatographic conditions are provided as Supporting Information (Table S2). Calibration curves were established by serial dilution in 50% acetonitrile to cover all expected concentrations in the samples. An amount of 20 μL from each dilution was mixed with 180 μL of blank matrix comprising blood, plasma, and brain homogenate. Since sufficient amounts of blank CSF could not be obtained; the calibration curve for the CSF was established in 10% plasma in saline to match the 10% plasma added to the CSF samples. For each sample (~1 mL) of plasma and brain homogenate, three to four 50 μL aliquots were protein-precipitated by adding 200 μL of cold acetonitrile. The same protein-precipitation was made with the single 50 μL CSF samples for each rat. The samples were vortexed for 2 min and then centrifuged (Rotanta/TR; Hettich, Tuttlingen, Germany) at 4000 rpm at 4 °C for 20 min. Then 75 μL of 0.2% formic acid and 75 μL of supernatant were transferred to a new 96-deep-well plate from which 5−20 μL samples were injected into the system.

2.2.5. Calculations. Unbound brain exposure was assessed as $K_{p,uu,brain}$, which is the ratio of the concentration of unbound drug in brain interstitial fluid ($C_{u,brainISF}$) to that in the plasma ($C_{u,p}$). $K_{p,uu,brain}$ was calculated by combining the total brain-to-plasma ratio $K_{p,brain}$ determined from in vivo samples (eq 1) with estimates of $V_{u,brain}$ and $f_{u,p}$ determined in vitro in brain slice and dialysis experiments (eq 2).

$$K_{p,brain} = \frac{A_{brain}}{C_p} \quad (1)$$

$$K_{p,uu,brain} = \frac{C_{u,brainISF}}{C_{u,p}} = \frac{K_{p,brain}}{V_{u,brain}\, f_{u,p}} \quad (2)$$

The amount of drug in the brain, A_{brain} (μmol/kg brain), also known as the total brain concentration, was calculated from the drug concentration in the brain homogenate using a correction method for drug in the residual blood of brain vascular spaces (eqs 3 and 4).[26]

$$A_{brain} = \frac{C_{brain,h} - C_p V_{eff}}{1 - V_{water}} \quad (3)$$

$$V_{eff} = f_{u,p} V_{water} + (1 - f_{u,p}) V_{protein} \quad (4)$$

$C_{brain,h}$ and C_p are the measured total drug concentrations in brain homogenate and plasma, respectively. V_{water} (10.3 μL/g brain) is the estimated vascular space of plasma water in residual blood. $V_{protein}$ (7.99 μL/g brain) is the apparent vascular space of plasma proteins. V_{eff} is the effective residual plasma volume, which is dependent on the plasma protein binding of the drug (eq 4).

As a potential surrogate for $K_{p,uu,brain}$, the ratio of the unbound concentration of drug in the CSF to that in plasma ($C_{u,CSF}/C_{u,p} = K_{p,uu,CSF}$) was calculated using the unbound CSF concentrations ($C_{u,CSF}$), calculated as the product of CSF concentrations (C_{CSF}) and the fraction of unbound drug in the CSF ($f_{u,CSF}$):

$$K_{p,uu,CSF} = \frac{C_{u,CSF}}{C_{u,p}} = \frac{C_{CSF}\, f_{u,CSF}}{C_{u,p}} \quad (5)$$

Since it was not feasible to obtain large volumes of rat CSF for equilibrium dialysis, $f_{u,CSF}$ was calculated from the unbound fraction in plasma using a single binding site model (eq 6) where the drug−protein dissociation constant was taken as the same in CSF and plasma.

$$f_{u,CSF} = \frac{1}{1 + Q_{alb}\left(\frac{1}{f_{u,p}} - 1\right)} \quad (6)$$

The albumin CSF to plasma ratio, Q_{alb}, was taken as 0.003 for rat cisternal CSF samples[27,28] and 0.005 for human lumbar samples.[22]

2.3. In Silico Models of Rat $K_{p,uu,brain}$ and $K_{p,brain}$. 2.3.1. Molecular Descriptors. Standard molecular descriptors were calculated: ClogP, ACDLogP, ACDLogD7.4, molecular weight (MW) and volume (VOL), number of rings (RingCount) and rotatable bonds (RotBond), van der Waals nonpolar (NPSA) and polar surface area (PSA), and the number of hydrogen bond donors (HBD) and acceptors (HBA) as defined by Lipinski. The pK_a of all drugs was accurately measured experimentally using capillary electrophoresis and mass spectromery.[29] The fraction of drug molecules that were un-ionized at pH 7.4 (LogUnionized) was calculated accordingly, and the drugs were classified as acid, base, neutral, or zwitterion according to the most abundant ion species at pH 7.4. ACDpKa was calculated and used for the drugs in the external data set (section 2.3.3). Calculated and measured molecular descriptors are given as Supporting Information (Table S3).

2.3.2. Development of in Silico Models. To find relationships between unbound brain exposure of the drug and the chemical structure of the drug, the multivariate PLS (projections to latent structures) method was applied using SIMCA P+[24] with default settings. PLS models for $K_{p,uu,brain}$ and $K_{p,brain}$ were developed on the basis of a training set comprising the original experimental in vivo data obtained using the brain slice method for all 43 drugs. $K_{p,uu,brain}$, $K_{p,brain}$, and the fraction un-ionized were log transformed prior to model development. To assess the importance of each variable, the linear coefficient of correlation (R^2) was calculated between log $K_{p,uu,brain}$ and log $K_{p,brain}$ and each of the 16 variables. To start with, all 16 descriptors were used in the development of PLS models; however, a variable selection procedure, in which groups of descriptors that did not contain information relevant to the problem (i.e., noise) were removed in a stepwise manner, was subsequently introduced to optimize and simplify the models. Descriptors were excluded from the model based on the variable importance for projection (VIP) score in SIMCA. The predictive performance of the new model was assessed according to the cross-validated coefficient of correlation[30] (Q^2). The variables were generally excluded up to the point where there was no improvement in Q^2 by further exclusion of variables.

2.3.3. External Model Validation. In addition to the internal cross-validation, an external validation of the PLS modeling was performed. Since the data were novel in terms of the methodology used (brain slice method, section 2.3.2), it was not possible to obtain a perfectly matching test set. The closest counterpart to the training set were data for $K_{p,uu,brain}$ from the literature, determined using brain homogenate binding in mice and rats or intracerebral microdialysis methods in rats. An extensive literature search resulted in 54 $K_{p,uu,brain}$ values determined by microdialysis (a total of 50 drugs) and 91 values determined by the homogenate method (a total of 74 drugs) (Supporting Information, Table S4). Model predictivity for this test set was assessed by the root of mean squared error of prediction (rmse). The significance of prediction bias was assessed using *t*-statistics.

2.4. Collection and Analysis of Human Data. The original clinical reports for the drugs selected from the Shen review[22] were retrieved, and additional literature searches were made for the remaining compounds. There were a total of 29 drugs for which drug concentrations in CSF had been measured in parallel with plasma concentrations, allowing a $K_{p,uu,CSF}$ to be calculated. The clinical reports were characterized in terms of the following: (1) the number of patients included, (2) the disease state of the patient, (3) whether a single dose or multiple doses had been administered, (4) the time after the last dose used for sampling, (5) the site of CSF sampling (lumbar/ventricular), and (6) whether the unbound fraction in plasma was determined. There were no consistent procedures for conducting the studies, although a typical case involved lumbar CSF sampling at a single time point 4 or more hours after the last of several doses. Since the unbound plasma concentration was rarely determined in the studies, it was decided to measure plasma protein binding in human plasma for all the compounds using the same equilibrium dialysis method as described in section 2.3.2. Regardless of any available data on $f_{u,p}$ (or $f_{u,CSF}$), the $f_{u,p}$ determined in this study was used to calculate the $K_{p,uu,CSF}$ from reported values of the total CSF-to-plasma ratio, using eq 6. There was more than one clinical report for a limited number of drugs; however, instead of taking an average, preference was given to the report which was, according to our judgment, more appropriately conducted in terms of sampling times, etc. The full details of the data set are provided as Supporting Information (Table S5).

3. Results and Discussion

3.1. Brain Exposure in the Rat. 3.1.1. Experimental Considerations. There was no difference ($p = 0.77$, *t* test) in the brain-to-plasma ratio of the permeability marker ^{14}C-sucrose when it was given in the two vehicles: saline (0.067 ± 0.045) and the mixture of dimethylacetamide, tetraethylene glycol, and water (0.075 ± 0.049). Similarly, there was no difference ($p = 0.81$) in the CSF-to-plasma ratio for ^{14}C-sucrose in saline (0.056 ± 0.023) versus the mixture (0.054 ± 0.015). These results indicate that the vehicles used in this study did not influence the passive transport properties of the BBB. Cassette dosing of up to three drugs was used to increase the number of compounds in the study despite the potential for interactions between the drugs at the BBB. The possibility that drug inhibition of Pgp may have affected the results of this study was assessed by comparing the observed unbound plasma concentrations (Table 1) with the in vitro potency of Pgp inhibition obtained from the literature. Taking the lowest reported values[31] for K_i or IC_{50}, the unbound plasma concentrations of verapamil and loperamide were lower than the IC_{50} by 5- and 46-fold, respectively. The concentrations of all other drugs stated to be Pgp inhibitors were lower than the IC_{50} by 200-fold or more. The use of in vitro K_i for prediction of Pgp-mediated drug interactions at the BBB is supported by in vivo experiments as well as by clinical findings.[32] Thus,

Table 1. Brain Exposure Ratios in the Rat[a] and Humans[b]

	rat							human data
	HBA	$C_{u,p}$ (μM)	$V_{u,brain}$ (mL/g brain)	$f_{u,p}$	$K_{p,brain}$	$K_{p,uu,brain}$	$K_{p,uu,,CSF}$	$K_{p,uu,,CSF}$
alprenolol	3	0.28	50	0.44	8.27	0.38	0.33	
amitriptyline	1	0.022	310	0.09	20.15	0.73	0.17	0.18
atenolol	5	1.5	2.5	1.0	0.07	0.026	0.036	0.54
baclofen	3	4.2	1.7	1.0	0.03	0.020	0.027	0.17
bupropion	2	0.079	16	0.31	9.78	2.00	0.49	2.0
cefotaxime	12	2.8	*c*	0.59	*c*	*c*	0.007	0.17
codeine	4	0.21	3.2	0.95	2.70	0.89	0.54	0.79
delavirdine	9	0.017	40	0.016	0.03	0.043	0.051	0.23
diazepam	3	0.061	20	0.12	2.28	1.07	0.78	0.79
diphenhydramine	2	0.051	32	0.48	16.25	1.05	0.39	
ethyl-phenylmalonamide	4	4.3	0.9	0.55	0.64	1.25	1.4	
gabapentin	3	5.2	4.6	1.0	0.64	0.14	0.067	0.16
indomethacin[f]	5	0.20	14	0.01	0.01	0.11	0.17	0.27
lamotrigine	5	1.8	4.6	0.51	2.02	0.88	0.86	1.10
levofloxacin	7	0.59	1.7	0.82	0.17	0.12	0.19	0.18
loperamide[f]	4	0.054	370	0.06	0.15	0.007	0.037	
M3G	10	2.7	0.60	1.00	0.007	0.011	0.049	0.081
M6G	10	2.1	0.99	0.98	0.008	0.008	0.017	0.10
methotrexate	13	2.9	0.68	1.00	0.004	0.006	0.007	0.062
metoprolol	4	0.75	5.5	0.90	3.14	0.64	0.43	0.93
morphine	4	0.23	3.7	0.90	0.51	0.15	0.40	0.51
moxalactam[f]	15	3.8	0.57	0.32	0.003	0.019	0.020	0.41
nadolol	5	0.78	3.4	0.86	0.11	0.037	0.041	
nelfinavir	7	0.0019	860	0.00	0.04	0.019	0.067	0.045
nitrofurantoin	9	0.71	1.6	0.48	0.008	0.011	0.0099	
norfloxacin	6	0.70	2.9	0.87	0.07	0.028	0.018	0.11
oxprenolol	4	0.21	11.8	0.45	1.06	0.20	0.10	
oxycodone	5	0.33	4.2	0.87	3.77	1.03	0.65	
oxymorphone	5	0.24	4.0	0.73	2.29	0.79	0.91	
paclitaxel	15	0.016	769	0.05	0.28	0.007	*d*	
pindolol	4	0.16	7.2	0.43	1.56	0.50	0.11	0.52
propranolol	3	0.051	118	0.09	6.59	0.61	0.49	0.42
rifampicin	16	0.83	6.9	0.12	0.03	0.035	0.34	2.2
salicylic acid	3	5.6	1.0	0.28	0.05	0.19	0.16	0.19
saquinavir	11	0.0030	208	0.007	0.08	0.055	*d*	0.096
sulphasalazine	9	0.013	4.2	0.005	0.002[e]	*e*	0.032	
tacrine	2	0.12	22	0.55	9.56	0.78	0.67	0.74
thiopental	4	0.55	4.3	0.19	1.28	1.53	1.09	0.75
thioridazine	2	0.0013	3333	0.002	3.75	0.45	0.21	1.4
topiramate	9	3.4	3.2	0.79	0.84	0.33	0.63	1.00
tramadol	3	0.30	4.2	0.85	5.29	1.46	0.71	1.44
verapamil	6	0.075	54	0.12	0.34	0.053	0.11	1.13
zidovudine	9	1.2	1.1	0.64	0.065	0.090	0.18	1.04

[a] Measured drug concentrations and standard deviations for all parameters are available as Supporting Information (Table S6). [b] References to and details of clinical reports are available as Supporting Information (Table S5). [c] Drug instability in brain homogenate. [d] Below limit of quantification. [e] Unacceptably large variability in K_p and $K_{p,uu}$ due to the correction made for drug in vascular spaces. [f] Data from Friden et al.[26]

the risk of Pgp inhibition by cassette dosing must be considered remote.

3.1.2. General Findings. The unbound brain-to-plasma concentration ratio $K_{p,uu,brain}$ was successfully determined in vivo for 41 of the 43 studied compounds (Table 1, Supporting Information Table S6). The range of $K_{p,uu,brain}$ was from 0.006 for methotrexate to 2.0 for buproprion, i.e., 300-fold. $K_{p,uu,brain}$ is interpreted in terms of drug efflux and influx, with values less than or greater than 1 indicating dominating drug efflux and influx, respectively. A $K_{p,uu,brain}$ value close to unity indicates the dominance of unrestricted and unfacilitated (passive) transport to the brain.[2] The overall importance of drug efflux at the BBB as a determinant of brain exposure is highlighted by 34 of 41 drugs having $K_{p,uu,brain}$ values less than unity and only 7 drugs having values slightly greater than unity. The total brain-to-plasma ratio, $K_{p,brain}$, also known as logBB, ranged from less than ~0.002 for sulfasalazine to 20 for amitriptyline, i.e., 10000-fold. This is a considerably larger range than that for $K_{p,uu,brain}$.

3.2. Structure−Brain Exposure Relationships in the Rat. 3.2.1. $K_{p,uu,brain}$. As discussed above, the only clinically useful predictions are those of unbound brain exposure, $K_{p,uu,brain}$. Development of global prediction models for $K_{p,uu,brain}$ is, however, inherently difficult because the model has to accommodate the sum of all drug interactions with transporters at the BBB as well as with the membrane, information that is not presently known. The present data

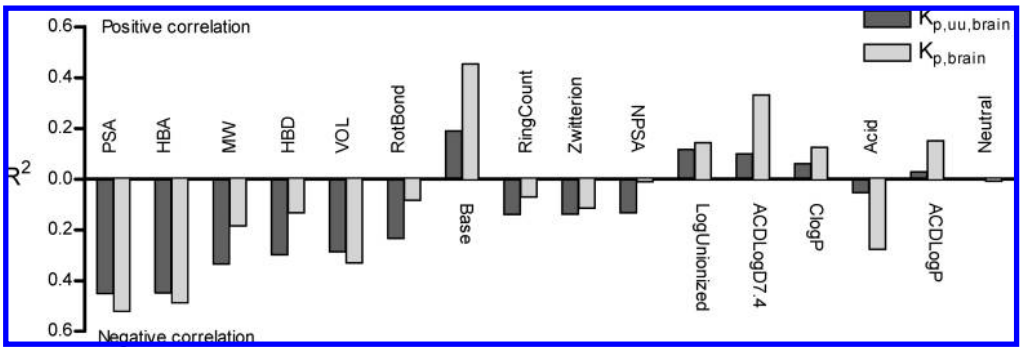

Figure 2. Linear correlation coefficient, R^2, for $K_{p,uu,brain}$, $K_{p,brain}$, and each of the 16 molecular descriptors for the selected drugs in the training data set. The upward and downward orientations of the bars represent positive and negative correlations, respectively, with $K_{p,uu,brain}$ and $K_{p,brain}$.

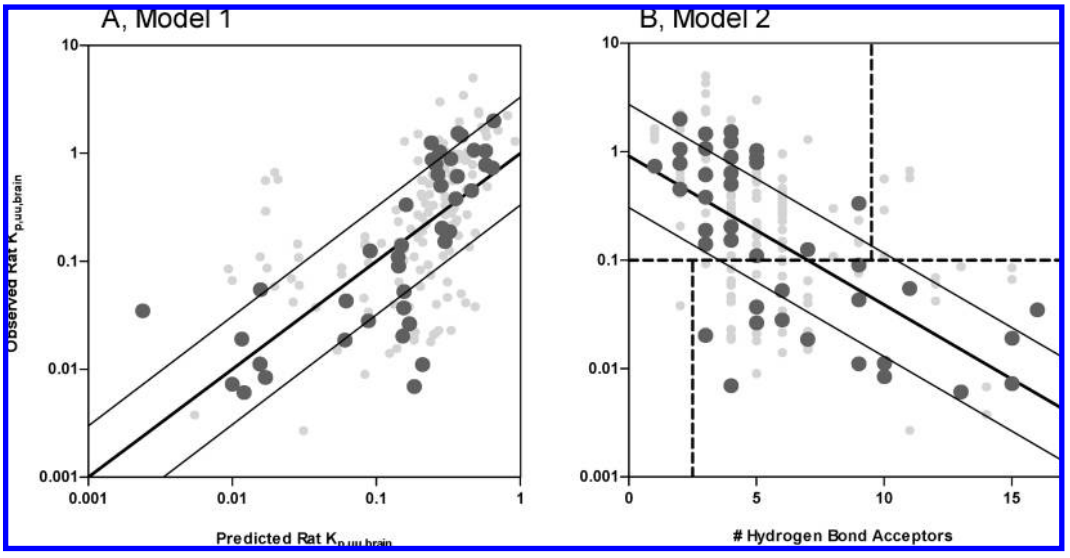

Figure 3. Observed versus predicted rat $K_{p,uu,brain}$ based on PLS 9 containing 16 molecular descriptors (A) and 10 using only the number of hydrogen acceptors (B). Large black filled circles are drugs in the training set. Small gray filled circles are observations from the external data set. Solid lines represent the prediction models, and fine lines represent a 3-fold error of prediction. Dashed lines in part B illustrate that drugs with no more than 2 HBA are very likely to have high unbound brain exposure and that drugs with 10 or more HBA are very likely to have low unbound brain exposure ($K_{p,uu,brain} < 0.1$).

Table 2. PLS Model Statistics

		training set				external set		
	parameter	descriptors	principal components	Q^2	rmse (x-fold)[a]	rmse (x-fold)[a]	bias[b]	p
model 1	$K_{p,uu,brain}$	all 16	1	0.452	3.48	3.99	1.22	0.11
model 2	$K_{p,uu,brain}$	HBA	1	0.426	3.94	4.19	1.29	0.03
model 3	$K_{p,brain}$ (logBB)	all 16	1	0.642	4.40			
model 4	$K_{p,brain}$ (logBB)	HBA, ACDLogD7.4, Acid, Base	1	0.693	3.99			

[a] Root of mean squared error analyzed on log scale. [b] Fold underprediction by model.

set contained drugs that are known substrates of drug transporters, many of which influence drug transport at the BBB, e.g., Pgp, BCRP, MRP1 (Supporting Information Table S1). Hence, at this point, the data can only be approached from the top down, using statistical tools to determine which properties are generally associated with a high or low $K_{p,uu,brain}$.

The most significant molecular descriptors for the relationship with unbound brain exposure were those that relate to hydrogen bonding, i.e., PSA and HBA (Figure 2). The first PLS model of $K_{p,uu,brain}$ (Figure 3A) used all 16 molecular descriptors simultaneously as variables and was also the model with the best predictivity ($Q^2 = 0.452$).

$$\log K_{p,uu,brain} = \begin{pmatrix} 0.17 - 0.00052\,MW + 0.015\,ACDLogD7.4 + 0.011\,ACDLogP + 0.015\,ClogP \\ -0.043\,HBD - 0.025\,HBA - 0.0016\,PSA - 0.00035\,NPSA - 0.00059\,VOL \\ -0.032\,RingCount - 0.017\,RotBond + 0.12\,Base - 0.11\,Acid - 0.0064\,Neurtral \\ -0.14\,Zwitterion + 0.026\,LogUnionized \end{pmatrix} \quad \text{(model 1)}$$

Model 1 did, however, contain a large number of variables that did not significantly contribute (Supporting Information Figure S2). Simplifications of the model were made by stepwise exclusion of less significant descriptors. Although the simplest models contained only descriptors of hydrogen bonding (PSA, HBA), they were almost equally predictive. Model 2 used HBA as the single descriptor ($Q^2 = 0.426$, Figure 3B, Table 2):

$$\log K_{p,uu,brain} = -0.04 - 0.14\,HBA \qquad \text{(model 2)}$$

Model 2 indicates that, in order to achieve a 2-fold increase in $K_{p,uu,brain}$, it is necessary to remove two HBAs. Conversely, a 2-fold reduction in $K_{p,uu,brain}$ can be achieved by addition of two HBAs. A change in $K_{p,uu,brain}$ as small as 2-fold can be considered significant since it principally means a doubling of the dose if the drug acts on a central target. If, on the other hand, there are critical CNS side effects associated with a peripherally acting drug, a reduction in $K_{p,uu,brain}$ by a factor 2 results in doubling the therapeutic window.

The data set of $K_{p,uu,brain}$ used for external validation was not established using the same methodology in rats; however, the data appear to be equally well predicted with little indication of bias (Figure 3, Table 2). The utility of a model for prioritizing between compounds in drug discovery can be evaluated by placing the average prediction error (~4-fold) in relation to the smallest change in $K_{p,uu,brain}$ that is of practical relevance (2-fold) while also considering the allowed range of variable values. The basic features (hydrogen bonding) of structure−brain exposure relationships were successfully revealed by the models and can be used as a default strategy for optimizing unbound brain exposure in drug discovery programs.

The Q^2 value of model predictivity provides the proportion of the variability in $K_{p,uu,brain}$ between drugs that was explained by the model. The presented models were capable of explaining only 40−45% of the variability in the training set. It follows, therefore, that approaches other than adding/removing HBA are required in order to fully maximize or minimize $K_{p,uu,brain}$. Strategies for improving model predictivity include the construction of local models that are specific to a particular class of drugs. However, the challenge of predicting the simultaneous influence of all known and unknown transporters at the BBB cannot be overestimated.

Simple rules of thumb are often used for a quick assessment of the likely level of brain exposure, given the structure of a molecule. A review of prediction models based on logBB showed that logBB will be high when the number of nitrogen (N) and oxygen (O) atoms in a molecule is equal to or less than 5 (HBA < 5) or when ClogP is numerically greater than the number of N + O atoms.[4] While it must be pointed out that brain exposure is a continuous variable, not an all-or-none response, the data from our study indicate that unbound brain exposure can generally be expected to be similar to systemic exposure ($K_{p,uu,brain} \approx 1$) only for drugs with as few as 2 HBA or N + O atoms (Figure 3B). An upper hydrogen bonding limit for peripherally restricted drugs cannot be defined because all drugs enter the brain to some extent.[33] However, this study indicates that brain exposure is likely to be at least 10-fold lower than systemic exposure ($K_{p,uu,brain} = 0.1$) if the number of HBAs is 10 or more (Figure 3B).

The mechanistic interpretation of HBA being the most important determinant should not be made using principles developed for oral drug absorption where the actual membrane permeability is crucial. Instead, for brain uptake, which is not similarly limited in time, only active transport mechanisms can prevent the drug from eventually equilibrating across the membrane and thus maintain a $K_{p,uu,brain}$ value different from unity. This is because the bulk flow of brain interstitial fluid is so small that it does not significantly contribute to the elimination of the vast majority of drugs.[2] This is evident from eq 7, expressing $K_{p,uu,brain}$ as a simplified function of inward (CL_{in}) and outward transport clearance (CL_{out}), which comprises passive transport ($CL_{passive}$), active efflux (CL_{efflux}), active influx (CL_{influx}), and elimination by brain interstitial fluid bulk flow ($CL_{bulkflow}$):

$$K_{p,uu,brain} = \frac{CL_{in}}{CL_{out}} = \frac{CL_{passive} + CL_{influx}}{CL_{passive} + CL_{efflux} + CL_{bulkflow}} \approx \frac{CL_{passive}}{CL_{passive} + CL_{efflux}} \qquad (7)$$

If CL_{influx} and $CL_{bulkflow}$ can be neglected, $K_{p,uu,brain}$ is composed of only $CL_{passive}$ and CL_{efflux} (eq 7). A question of fundamental interest is then whether the relationship seen between $K_{p,uu,brain}$ and hydrogen bonding is due to the effect on passive transport or whether both passive transport and active transport are involved. An isolated effect on passive transport appears unlikely, since it would imply a basal level of efflux for all drugs. Active efflux is possibly also promoted by hydrogen bonding due to increased interaction possibilities (hydrogen bonds), important for efflux transporters such as Pgp.[34] A double role for hydrogen bonding is implied by the necessity for solvation hydrogen bond breakage before entering the membrane and binding to Pgp in the hydrophobic environment of the membrane. Interestingly, lipophilicity, which is normally correlated with passive transport, did not increase the value of $K_{p,uu,brain}$ in this study. It is likely that the effect of increased passive transport ($CL_{passive}$) by increased lipophilicity is paralleled and offset by increased efflux (CL_{efflux}), owing to increased drug concentrations in the membrane where the interaction with the efflux transporter takes place. Hence, the dominating position of hydrogen bonding for structure−brain exposure relationships seems to arise from its additive effects on passive and active transport independently of lipophilicity: a less lipophilic drug with many HBAs has very limited passive transport and is thus sensitive to low capacity active efflux (eq 7), while a lipophilic drug with many HBAs is a probable transporter substrate, e.g., a Pgp substrate.[35]

3.2.3. $K_{p,brain}$ (logBB). $K_{p,brain}$ or logBB is a hybrid parameter that contains information on brain exposure ($K_{p,uu,brain}$) in a form that is distorted by plasma protein and tissue binding, neither of which are relevant to unbound brain exposure per se:

$$BB = K_{p,uu,brain}\, V_{u,brain}\, f_{u,p} \qquad (8)$$

Because of the long history of logBB use and in order to compare it with $K_{p,uu,brain}$, the relationship between the chemical structure of the drug and logBB was also investigated. As for $K_{p,uu,brain}$, the relationship is dominated by hydrogen bonding, but in contrast to $K_{p,uu,brain}$, logBB is also positively correlated with lipophilicity. Furthermore, logBB is higher for basic drugs than for acidic drugs (Figure 2). The PLS model that was developed contained a descriptor for hydrogen bonding (HBA), lipophilicity (ACDLogD7.4), and the ion class of the drug (acid or base) (model 4, Table 2):

$$\log BB = -0.18 - 0.097\,HBA + 0.10\,ACDLogD7.4 + 0.68\,Base - 0.67\,Acid \qquad \text{(model 4)}$$

The mechanistic interpretation of 11 is straightforward: HBA accounts for the part of logBB which is related to brain exposure ($K_{p,uu,brain}$, eq 8); ACDLogD7.4 and the drug being basic

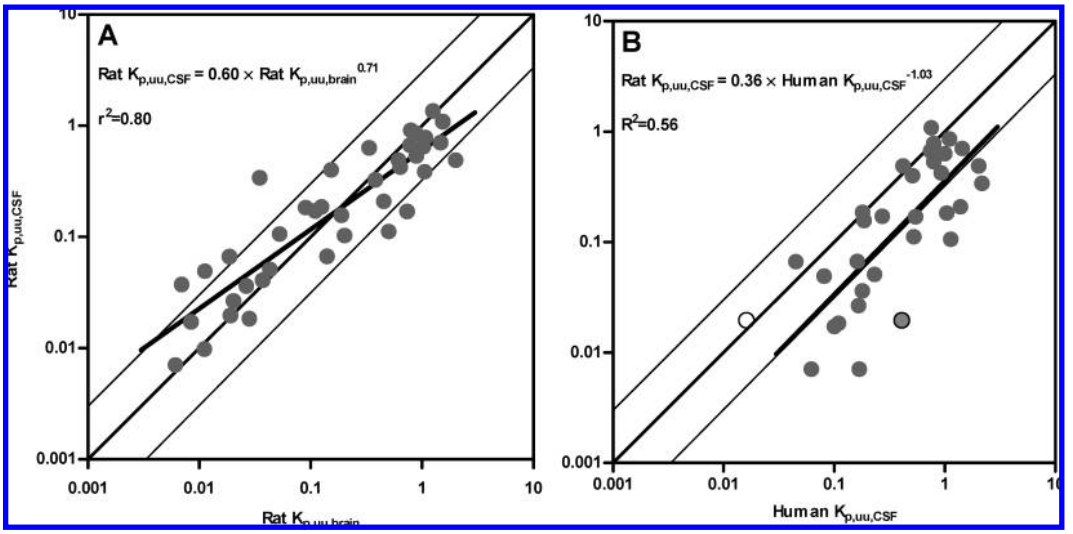

Figure 4. Relationship between $K_{p,uu,CSF}$ and $K_{p,uu,brain}$ in the rat (A) and the agreement between rat and human $K_{p,uu,CSF}$ (B). Fine lines represent identity and 3-fold differences. Solid lines are the result of linear regression analysis of log-transformed data. Data points represent average values for one drug. Moxalactam (circles) was included from both a study in patients with bacterial meningitis (filled circle) and a study in healthy volunteers (open circle) (B).

account for binding to phospholipid in tissue[36] ($V_{u,brain}$, eq 8); and the drug being acidic accounts for extensive binding to albumin in plasma ($f_{u,p}$, eq 8). The relatively better predictivity of 11 (Q^2 = 0.693) provides no incentive to actually use it for drug design. In fact, doing so results in the design of drug compounds that are unnecessarily lipophilic or basic without improved pharmacodynamics.

3.3. Relationship between $K_{p,uu,CSF}$ and $K_{p,uu,brain}$ in the Rat. Historically, the drug concentration in cerebrospinal fluid has been regarded as being in equilibrium with the concentration at central target sites.[37] Therefore, CSF sampling has been a procedure for assessing the availability of drugs to targets within the CNS. The contemporary view, however, is that the CSF compartment is separate from the interstitial fluid of the brain tissue.[38] While this cannot be disputed from an anatomical or physiological perspective, the question of importance for drug discovery is whether the level of drug protection provided by the BBB and the BCSFB is similar enough to allow the use of the CSF as a surrogate measure of brain exposure.[17,39] The data collected in this study allowed a direct comparison of unbound CSF vs ISF concentrations normalized to unbound plasma concentrations, i.e., $K_{p,uu,CSF}$ vs $K_{p,uu,brain}$, in the rat (Figure 4A, Table 1). $K_{p,uu,CSF}$ was within 3-fold of $K_{p,uu,brain}$ for 33 of 39 drugs, which is a striking agreement given the physiological differences and the range of observations covering almost 3 orders of magnitude. In principle, these results support the use of $K_{p,uu,CSF}$ for cross-species comparison of brain exposure data (section 3.4).

There was, however, an overall tendency for CSF data to overpredict $K_{p,uu,brain}$ for drugs with low $K_{p,uu,brain}$ and to underpredict for drugs with higher $K_{p,uu,brain}$ (Figure 4A). This suggests that the efflux capacity of the BCSFB is lower than that of the BBB, which could be related to Pgp being oriented at the BCSFB such that its substrates are influxed into the CSF[40−42] or that efflux functioning of Pgp at the BCSF is minimal or less efficient relative to that at the BBB. Notably, overprediction was seen for the Pgp substrates in this data set: verapamil, loperamide, rifampicin, and nelfinavir (Figure 4A). Given the importance of Pgp at the BBB, care should be taken not to overestimate brain exposure of Pgp substrates from measurements of $K_{p,uu,CSF}$. The underprediction for drugs with higher $K_{p,uu,brain}$ is intriguing and could be related to less efficient drug influx at the BCSFB in comparison with that at the BBB. Alternatively, the BCSFB lacks the influx transporters of the BBB. If active influx at the BBB, but not at the BCSFB, was the reason for underprediction, one might have expected values for $K_{p,uu,brain}$ to be greater than unity. However, active influx and active efflux transport often occur simultaneously and can result in any value for $K_{p,uu,brain}$ or $K_{p,uu,CSF}$. The group for which $K_{p,uu,CSF}$ underpredicted a high $K_{p,uu,brain}$ mainly comprised basic drugs. This could indicate differences in the expression or function of organic cation transporters (OCTs) at the BBB and BCSFB. Oxycodone, which was previously shown to be actively influxed at the BBB, belonged to this group.[1,43]

The regression line of Figure 3A could principally be used for conversion of $K_{p,uu,CSF}$ to $K_{p,uu,brain}$; however, the slope of the relationship, which was less than unity (0.6), implies that drugs with diverging values of $K_{p,uu,brain}$ are paralleled by a narrower rang of values for $K_{p,uu,CSF}$. Hence, $K_{p,uu,CSF}$ is a rather "insensitive" surrogate measure of $K_{p,uu,brain}$. Nevertheless, $K_{p,uu,CSF}$ can provide some information on unbound brain exposure when it is not possible to measure $K_{p,uu,brain}$, which is generally the case in human patients. More data need to be collected to further compare substance properties regarding active efflux or influx at the BBB with CSF information.

3.4. Agreement between Rat and Human $K_{p,uu,CSF}$. The relevance to humans of structure−brain exposure relationships in the rat was evaluated by comparing $K_{p,uu,CSF}$ determined in rats and human patients (Figure 4B). The rank order of the drugs was similar, and given the magnitude of normal experimental variability and the diversity of collected human data, a reasonable relationship was seen between rat and human $K_{p,uu,CSF}$ (r^2 = 0.55). There was, however, a bias toward the observed human $K_{p,uu,CSF}$ values being on average 3-fold higher than the corresponding values in the rat. This bias could be due to rats having developed CNS barriers capable of providing a higher level of protection from exogenous compounds than humans. Such species

differences were seen in a recent PET study where $K_{p,brain}$ of different Pgp substrates was determined in different species.[44] The turnover half-life of CSF in humans (170 min) is longer than in rats (40−100 min),[45] which conceivably contributes to the apparent species difference in $K_{p,uu,CSF}$. A difference in $K_{p,uu,CSF}$ due to CSF turnover does not, however, imply a difference in $K_{p,uu,brain}$, since the bulk flow of brain interstitial fluid has an even longer half-life (14 h)[46] and is believed to be of little importance for the elimination of most druglike molecules.[2]

While the biological explanations discussed above are plausible, there are three principal experimental factors that also contribute to the observed $K_{p,uu,CSF}$ species difference: (1) the disease state of the patients, (2) kinetic bias due to timing of CSF sampling, and (3) the different CSF sources used for rat (cisternal) and human (lumbar). First, and most importantly, the subjects of the clinical reports were typically not healthy volunteers but patients with various disease states (Table S4). Several of these diseases, such as hypertension, multiple sclerosis, meningitis, traumatic brain injury, Alzheimer's disease, and HIV infection, are known to be associated with alterations in CNS barrier function.[47] The quantitative impact on $K_{p,uu,CSF}$ is unclear, although some indication is provided by moxalactam, for which the $K_{p,uu,CSF}$ was 25-fold lower in healthy volunteers than in patients with bacterial meningitis (Figure 4B). Furthermore, an increased CSF-to-plasma albumin concentration ratio is seen in many neurological disorders as a consequence of reduced CSF turnover.[48] In the data utilized in the present study, the albumin CSF-to-plasma ratio was not measured in each patient and a standard value from healthy subjects was used for calculation of $K_{p,uu,CSF}$. Hence, human $K_{p,uu,CSF}$ was potentially overestimated for highly protein-bound drugs in this study.

The second experimental reason for the observed rat/human $K_{p,uu,CSF}$ difference may be a delay in appearance and elimination of drug in the CSF relative to plasma, which makes the dosage regimen and the timing of CSF sampling critical. Ideally, the CSF and plasma would be sampled simultaneously at steady state during continuous intravenous infusion or alternatively at several time points following a single dose. This was rarely performed in humans, and since the single CSF sample was generally taken several hours after the last dose, it is almost certain that a kinetic bias was introduced for higher values of $K_{p,uu,CSF}$. This is contrasted by the rat experiments, where 4 h intravenous infusions were given to rats to approach steady state and where $K_{p,uu,CSF}$ would be underestimated for any drug for which 4 h was not sufficient to attain complete equilibrium.

Third, $K_{p,uu,CSF}$ was determined using CSF samples from cisterna magna in the rat and generally by lumbar puncture in the patients. The impact of different sampling sites on the $K_{p,uu,CSF}$ comparison will depend on the extent of drug exchange between the CSF and the blood via the blood−spinal cord barrier and cord tissue along the path of CSF flow. Although the blood−spinal cord barrier is similar to the BBB in terms of cellular structure, its permeability is generally higher than that of the BBB.[49] Therefore, the value of $K_{p,uu,CSF}$ is expected to be higher from lumbar samples if there is significant drug exchange with blood across the blood−spinal cord barrier. If, on the other hand, drug exchange is not significant, lumbar CSF would reflect cranial CSF with a lag time of 60−90 min,[50] thus potentiating the kinetic bias discussed above. Either way, given the general timing of CSF sampling in the clinical material, human $K_{p,uu,CSF}$ from the lumbar sampling site is expected to be overestimated to some extent relative to the rat.

The comparison of $K_{p,uu,CSF}$ in the rat and humans confirms that there is a viable relationship between the species with respect to brain exposure, thus justifying the use of the rat for the study of central drug exposure. However, because of insufficient control of experimental factors for the human data set in particular, it is very difficult to assess the strength of the relationship or to conclude whether the observed 3-fold difference reflects a true species difference, an observational bias, or both.

4. Conclusions

The recent development of experimental methods has facilitated the generation of a reasonably sized (n = 43), structurally diverse data set describing unbound and pharmacologically active brain exposure to drugs in the rat. The data set, which is presented in this study, was used to evaluate the relationship between molecular structure and unbound brain exposure. Molecular descriptors related to hydrogen bonding dominated the relationship because of the additive effect of reducing passive permeation while increasing the possibility of interactions with efflux transporters. In contrast to previous reports based on the total brain-to-plasma ratio (logBB), lipophilicity was not correlated with unbound brain exposure, which is a finding with immediate implications for drug design. The simplest and most attractive model predicts that the addition of 2 HBAs to the structure of a centrally acting drug results in a 2-fold reduction of unbound brain exposure and hence doubled dosage requirements. On the other hand, the addition of 2 HBAs to a peripherally acting drug with critical CNS side effects will result in a beneficial doubling of the therapeutic window. Since active transport mediated by a panel of transporters at the BBB determines unbound brain exposure, the modest predictivity of the developed PLS models was not surprising. Construction of local PLS models for specific drug groups may improve predictivity; however, successful prediction is likely to depend on the development of in silico models that specifically address the interactions with various drug transporters.

There was a similar rank order between drugs with respect to $K_{p,uu,brain}$ and $K_{p,uu,CSF}$ and a within 3-fold agreement for 33 of 39 drugs. Deviations from agreement were interpreted as BCSFB having lower efficiency of both active drug efflux and active influx compared to the BBB. We conclude that $K_{p,uu,CSF}$ is a fairly good surrogate measure of unbound brain exposure; however, for studies in small animals, $K_{p,uu,brain}$ is just as easily measured using a combination of tissue sampling at steady state and the brain slice method.

The relevance to humans of structure−brain exposure relationships in the rat was evaluated by comparing $K_{p,uu,CSF}$ obtained from clinical studies and corresponding measurements in rats. The 3-fold difference between human and rat $K_{p,uu,CSF}$ could be related to a number of experimental factors but may also in part represent a real species difference. Most importantly, the rank order of the drugs was similar for human and rat $K_{p,uu,CSF}$ values, a finding that provides experimental support for applying structure−brain exposure relationships derived from the rat to drug design.

Supporting Information Available: Chemical structures of the drugs (Figure S1), plot of variable importance for projections of model 1 (Figure S2), list of human transporters for which the drugs

are substrates (Table S1), bioanalytical methods (Table S2), calculated and measured molecular descriptors (Table S3), external data set of $K_{p,uu,brain}$ with references (Table S4), detailed data on $K_{p,uu,CSF}$ in patients with references (Table S5), and detailed data of $K_{p,brain}$, $K_{p,uu,brain}$, and $K_{p,uu,CSF}$ in rats (Table S6). This material is available free of charge via the Internet at http://pubs.acs.org.

References

(1) Bostrom, E.; Simonsson, U.; Hammarlund-Udenaes, M. In vivo blood−brain barrier transport of oxycodone in the rat: indications of active influx and implications for PK/PD. *Drug Metab. Dispos.* **2006**, *34*, 1624–1631.

(2) Hammarlund-Udenaes, M.; Friden, M.; Syvanen, S.; Gupta, A. On the rate and extent of drug delivery to the brain. *Pharm. Res.* **2008**, *25*, 1737–1750.

(3) Kelder, J.; Grootenhuis, P. D.; Bayada, D. M.; Delbressine, L. P.; Ploemen, J. P. Polar molecular surface as a dominating determinant for oral absorption and brain penetration of drugs. *Pharm. Res.* **1999**, *16*, 1514–1519.

(4) Norinder, U.; Haeberlein, M. Computational approaches to the prediction of the blood−brain distribution. *Adv. Drug Delivery Rev.* **2002**, *54*, 291–313.

(5) Seelig, A.; Gottschlich, R.; Devant, R. M. A method to determine the ability of drugs to diffuse through the blood−brain barrier. *Proc. Natl. Acad. Sci. U.S.A.* **1994**, *91*, 68–72.

(6) van de Waterbeemd, H.; Camenisch, G.; Folkers, G.; Chretien, J. R.; Raevsky, O. A. Estimation of blood−brain barrier crossing of drugs using molecular size and shape, and H-bonding descriptors. *J. Drug Targeting* **1998**, *6*, 151–165.

(7) Hammarlund-Udenaes, M.; Bredberg, U.; Friden, M. Methodologies to assess brain drug delivery in lead optimization. *Curr. Top. Med. Chem.* **2009**, *9*, 148–162.

(8) Pardridge, W. M. Log(BB), PS products and in silico models of drug brain penetration [comment]. *Drug Discovery Today* **2004**, *9*, 392–393.

(9) Mano, Y.; Higuchi, S.; Kamimura, H. Investigation of the high partition of YM992, a novel antidepressant, in rat brain: in vitro and in vivo evidence for the high binding in brain and the high permeability at the BBB. *Biopharm. Drug Dispos.* **2002**, *23*, 351–360.

(10) Kalvass, J. C.; Maurer, T. S. Influence of nonspecific brain and plasma binding on CNS exposure: implications for rational drug discovery. *Biopharm. Drug Dispos.* **2002**, *23*, 327–338.

(11) Friden, M.; Ducrozet, F.; Antonsson, M.; Middleton, B.; Bredberg, U.; Hammarlund-Udenaes, M. Development of a high-throughput brain slice method for studying drug distribution in the CNS. *Drug Metab. Dispos.* **2009**, *37*, 1226.

(12) Friden, M.; Gupta, A.; Antonsson, M.; Bredberg, U.; Hammarlund-Udenaes, M. In vitro methods for estimating unbound drug concentrations in the brain interstitial and intracellular fluids. *Drug Metab. Dispos.* **2007**, *35*, 1711–1719.

(13) Becker, S.; Liu, X. Evaluation of the utility of brain slice methods to study brain penetration. *Drug Metab. Dispos.* **2006**, *34*, 855–861.

(14) Liu, X.; Chen, C. Strategies to optimize brain penetration in drug discovery. *Curr. Opin. Drug Discovery Dev.* **2005**, *8*, 505–512.

(15) Kalvass, J. C.; Maurer, T. S.; Pollack, G. M. Use of plasma and brain unbound fractions to assess the extent of brain distribution of 34 drugs: comparison of unbound concentration ratios to in vivo p-glycoprotein efflux ratios. *Drug Metab. Dispos.* **2007**, *35*, 660–666.

(16) Kalvass, J. C.; Olson, E. R.; Pollack, G. M. Pharmacokinetics and pharmacodynamics of alfentanil in P-glycoprotein-competent and P-glycoprotein-deficient mice: P-glycoprotein efflux alters alfentanil brain disposition and antinociception. *Drug Metab. Dispos.* **2007**, *35*, 455–459.

(17) Liu, X.; Smith, B. J.; Chen, C.; Callegari, E.; Becker, S. L.; Chen, X.; Cianfrogna, J.; Doran, A. C.; Doran, S. D.; Gibbs, J. P.; Hosea, N.; Liu, J.; Nelson, F. R.; Szewc, M. A.; Van Deusen, J. Evaluation of cerebrospinal fluid concentration and plasma free concentration as a surrogate measurement for brain free concentration. *Drug Metab. Dispos.* **2006**, *34*, 1443–1447.

(18) Summerfield, S. G.; Read, K.; Begley, D. J.; Obradovic, T.; Hidalgo, I. J.; Coggon, S.; Lewis, A. V.; Porter, R. A.; Jeffrey, P. Central nervous system drug disposition: the relationship between in situ brain permeability and brain free fraction. *J. Pharmacol. Exp. Ther.* **2007**, *322*, 205–213.

(19) Summerfield, S. G.; Stevens, A. J.; Cutler, L.; del Carmen Osuna, M.; Hammond, B.; Tang, S. P.; Hersey, A.; Spalding, D. J.; Jeffrey, P. Improving the in vitro prediction of in vivo central nervous system penetration: integrating permeability, P-glycoprotein efflux, and free fractions in blood and brain. *J. Pharmacol. Exp. Ther.* **2006**, *316*, 1282–1290.

(20) Maurer, T. S.; Debartolo, D. B.; Tess, D. A.; Scott, D. O. Relationship between exposure and nonspecific binding of thirty-three central nervous system drugs in mice. *Drug Metab. Dispos.* **2005**, *33*, 175–181.

(21) Doran, A.; Obach, R. S.; Smith, B. J.; Hosea, N. A.; Becker, S.; Callegari, E.; Chen, C.; Chen, X.; Choo, E.; Cianfrogna, J.; Cox, L. M.; Gibbs, J. P.; Gibbs, M. A.; Hatch, H.; Hop, C. E.; Kasman, I. N.; Laperle, J.; Liu, J.; Liu, X.; Logman, M.; Maclin, D.; Nedza, F. M.; Nelson, F.; Olson, E.; Rahematpura, S.; Raunig, D.; Rogers, S.; Schmidt, K.; Spracklin, D. K.; Szewc, M.; Troutman, M.; Tseng, E.; Tu, M.; Van Deusen, J. W.; Venkatakrishnan, K.; Walens, G.; Wang, E. Q.; Wong, D.; Yasgar, A. S.; Zhang, C. The impact of P-glycoprotein on the disposition of drugs targeted for indications of the central nervous system: evaluation using the MDR1A/1B knockout mouse model. *Drug Metab. Dispos.* **2005**, *33*, 165–174.

(22) Shen, D. D.; Artru, A. A.; Adkison, K. K. Principles and applicability of CSF sampling for the assessment of CNS drug delivery and pharmacodynamics. *Adv. Drug Delivery Rev.* **2004**, *56*, 1825–1857.

(23) Skold, C.; Winiwarter, S.; Wernevik, J.; Bergstrom, F.; Engstrom, L.; Allen, R.; Box, K.; Comer, J.; Mole, J.; Hallberg, A.; Lennernas, H.; Lundstedt, T.; Ungell, A. L.; Karlen, A. Presentation of a structurally diverse and commercially available drug data set for correlation and benchmarking studies. *J. Med. Chem.* **2006**, *49*, 6660–6671.

(24) *SIMCA P+*, version 11.5; Umetrics, AB (Box 7960, SE-90717 Umeå, Sweden), 2006.

(25) Wan, H.; Rehngren, M. High-throughput screening of protein binding by equilibrium dialysis combined with liquid chromatography and mass spectrometry. *J. Chromatogr., A* **2006**, *1102*, 125–134.

(26) Friden, M.; Ljungqvist, H.; Middleton, B.; Bredberg, U.; Hammarlund-Udenaes, M. Improved measurement of drug exposure in brain using drug-specific correction for residual blood. *J.Cereb. Blood Flow Metab.*, in press.

(27) Crowe, A.; Morgan, E. H. Iron and transferrin uptake by brain and cerebrospinal fluid in the rat. *Brain Res.* **1992**, *592*, 8–16.

(28) Habgood, M. D.; Sedgwick, J. E.; Dziegielewska, K. M.; Saunders, N. R. A developmentally regulated blood−cerebrospinal fluid transfer mechanism for albumin in immature rats. *J. Physiol.* **1992**, *456*, 181–192.

(29) Wan, H.; Holmen, A. G.; Wang, Y.; Lindberg, W.; Englund, M.; Nagard, M. B.; Thompson, R. A. High-throughput screening of pK_a values of pharmaceuticals by pressure-assisted capillary electrophoresis and mass spectrometry. *Rapid Commun. Mass Spectrom.* **2003**, *17*, 2639–2648.

(30) Wold, S. Validation of QSAR's. *Quant. Struct.−Act. Relat.* **1991**, *10*, 191–193.

(31) TP-search. www.tp-search.jp.

(32) Hsiao, P.; Bui, T.; Ho, R. J.; Unadkat, J. D. In vitro-to-in vivo prediction of P-glycoprotein-based drug interactions at the human and rodent blood−brain barrier. *Drug Metab. Dispos.* **2008**, *36*, 481–484.

(33) Fagerholm, U. The highly permeable blood−brain barrier: an evaluation of current opinions about brain uptake capacity. *Drug Discovery Today* **2007**, *12*, 1076–1082.

(34) Seelig, A. A general pattern for substrate recognition by P-glycoprotein. *Eur. J. Biochem.* **1998**, *251*, 252–261.

(35) Seelig, A.; Landwojtowicz, E. Structure−activity relationship of P-glycoprotein substrates and modifiers. *Eur. J. Pharm. Sci.* **2000**, *12*, 31–40.

(36) Wan, H.; Rehngren, M.; Giordanetto, F.; Bergstrom, F.; Tunek, A. High-throughput screening of drug−brain tissue binding and in silico prediction for assessment of central nervous system drug delivery. *J. Med. Chem.* **2007**, *50*, 4606–4615.

(37) Danhof, M.; Levy, G. Kinetics of drug action in disease states. I. Effect of infusion rate on phenobarbital concentrations in serum, brain and cerebrospinal fluid of normal rats at onset of loss of righting reflex. *J. Pharmacol. Exp. Ther.* **1984**, *229*, 44–50.

(38) de Lange, E. C.; Danhof, M. Considerations in the use of cerebrospinal fluid pharmacokinetics to predict brain target concentrations in the clinical setting: implications of the barriers between blood and brain. *Clin. Pharmacokinet.* **2002**, *41*, 691–703.

(39) Lin, J. H. CSF as a surrogate for assessing CNS exposure: an industrial perspective. *Curr. Drug Metab.* **2008**, *9*, 46–59.

(40) Kusuhara, H.; Sugiyama, Y. Efflux transport systems for drugs at the blood−brain barrier and blood−cerebrospinal fluid barrier (Part 1). *Drug Discovery Today* **2001**, *6*, 150–156.

(41) Sugiyama, Y.; Kusuhara, H.; Suzuki, H. Kinetic and biochemical analysis of carrier-mediated efflux of drugs through the blood−brain and blood−cerebrospinal fluid barriers: importance in the drug delivery to the brain. *J. Controlled Release* **1999**, *62*, 179–186.

(42) Rao, V. V.; Dahlheimer, J. L.; Bardgett, M. E.; Snyder, A. Z.; Finch, R. A.; Sartorelli, A. C.; Piwnica-Worms, D. Choroid plexus epithelial expression of MDR1 P glycoprotein and multidrug resistance-associated protein contribute to the blood−cerebrospinal-fluid drug-permeability barrier. *Proc. Natl. Acad. Sci. U.S.A.* **1999**, *96*, 3900–3905.
(43) Okura, T.; Hattori, A.; Takano, Y.; Sato, T.; Hammarlund-Udenaes, M.; Terasaki, T.; Deguchi, Y. Involvement of the pyrilamine transporter, a putative organic cation transporter, in blood−brain barrier transport of oxycodone. *Drug Metab. Dispos.* **2008**, *36*, 2005–2013.
(44) Syvanen, S.; Lindhe, O.; Palner, M.; Kornum, B. R.; Rahman, O.; Langstrom, B.; Knudsen, G. M.; Hammarlund-Udenaes, M. Species differences in blood−brain barrier transport of three positron emission tomography radioligands with emphasis on P-glycoprotein transport. *Drug Metab. Dispos.* **2009**, *37*, 635–643.
(45) Davson, H.; Segal, M. B. *Physiology of the CSF and Blood−Brain Barrier*; CRC Press: Boca Raton, FL, 1995.
(46) Abbott, N. J. Evidence for bulk flow of brain interstitial fluid: significance for physiology and pathology. *Neurochem. Int.* **2004**, *45*, 545–552.
(47) Pardridge, W. M. *Introduction to the Blood−Brain Barrier*; Cambridge University Press: Cambridge, U.K., 1998; pp 1−162.
(48) Reiber, H.; Peter, J. B. Cerebrospinal fluid analysis: disease-related data patterns and evaluation programs. *J. Neurol. Sci.* **2001**, *184*, 101–122.
(49) Neuwelt, E.; Abbott, N. J.; Abrey, L.; Banks, W. A.; Blakley, B.; Davis, T.; Engelhardt, B.; Grammas, P.; Nedergaard, M.; Nutt, J.; Pardridge, W.; Rosenberg, G. A.; Smith, Q.; Drewes, L. R. Strategies to advance translational research into brain barriers. *Lancet Neurol.* **2008**, *7*, 84–96.
(50) Chiro, G. D.; Hammock, M. K.; Bleyer, W. A. Spinal descent of cerebrospinal fluid in man. *Neurology* **1976**, *26*, 1–8.